

The Source of Maser Emission in W33C (G12.8–0.2)

P. Colom¹, E. E. Lekht^{2*}, M. I. Pashchenko², and G. M. Rudnitskii²

¹LESIA, Observatoire de Paris—Meudon, 5 Place Jules Janssen, 92195 Meudon Cedex, France

²Lomonosov Moscow State University, Sternberg Astronomical Institute,
Universitetskii prospekt 13, Moscow, 119234 Russia

Received January 18, 2012; in final form, March 2, 2012

Abstract—The results of observations of the H₂O and OH maser sources toward the region of W33C (G12.8–0.2) are reported. The observations were carried out on the 22-m radio telescope of the Pushchino Radio Astronomy Observatory in the 1.35-cm water-vapor line and on the Large Radio Telescope at Nançay (France), in the main (1665 and 1667 MHz) and satellite (1612 and 1720 MHz) OH lines. Multiple, strongly variable, short-lived H₂O emission features were detected in a broad interval of radial velocities, from –7 to 55 km/s. OH maser emission in the 1667-MHz line was detected at velocities of 35–41 km/s. The Stokes parameters of the maser emission in the main OH lines 1665 and 1667 MHz were measured. Zeeman splitting was detected in the 1665-MHz line at 33.4 and 39.4 km/s, and in the 1667 MHz line only at 39.4 km/s. The magnetic-field intensity was estimated. Appreciable variability of the Zeeman splitting components was observed at 39 and 39.8 km/s in both main lines. The extended spectrum and fast variability of the H₂O maser emission, together with the variability of the Zeeman-splitting components in the main OH lines, may indicate a composite clumpy structure of the molecular cloud and the presence of large-scale rotation, bipolar outflows, and turbulent motions of material in this cloud.

DOI: 10.1134/S1063772912100034

1. INTRODUCTION

The maser radio emission in the OH lines toward the HII region in W33C (G12.8–0.2) was detected by Pashchenko in 1975 [1, 2], and emission in the 1.35-cm water-vapor line by Genzel and Downes in 1976 [3].

The radio continuum source in this region has two emission peaks. Observations at 408 MHz [4] and 5000 MHz [5] showed that the fainter component, G12.7–0.2, is 5' × 4' in size, while the size of the intense component, G12.8–0.2, is only 0.8'. The kinematic distance to G12.8–0.2 was estimated from the neutral-hydrogen absorption line profile to be 5 kpc [6].

In January 1975 and October 1978, we carried out observations toward the continuum source W33C on the Large Radio Telescope in Nançay (France) in all four 18-cm OH lines, in both circular polarizations [1, 2]. Strongly polarized maser emission at velocities of 32.5 and 34.5 km/s was detected in the main 1665-MHz OH line against the background of strong absorption toward the HII region G12.8–0.2. We observed faint emission in the 1667-MHz line, also against the background of strong

absorption. We also determined the coordinates of the OH emission source to be $\alpha_{1950} = 18^{\text{h}}11^{\text{m}}18.5^{\text{s}}$, $\delta_{1950} = -17^{\circ}56' \pm 1.5'$. The OH maser is embedded in a compact molecular cloud, which is a source of type IIc OH emission in the 1612- and 1720-MHz satellite lines.

Subsequently, we conducted observations of the W33C OH maser in 1991 and 2008–2011. Unfortunately, there is no information about observations of this OH maser by other authors in the literature, either using single dishes or high angular resolution systems. Note that the W33 region hosts two centers of 1665-MHz maser emission arranged symmetrically on either side of W33C.

In November 1976, Genzel and Downes [3] detected intense H₂O maser emission from W33C at 1.35 cm on the 100-m radio telescope in Effelsberg at radial velocities from –4 to 1 km/s (8 Jy), as well as weaker emission (less than 4 Jy) at velocities from 30 to 41 km/s. The coordinates of the detected source coincided with those of the OH maser source to within the errors. The W33C H₂O maser was later observed by Jaffe et al. [7] and Comoretto et al. [8]. In 1981, the emission was notably weaker and occurred at –7 and 34 km/s.

*E-mail: lekht@sai.msu.ru

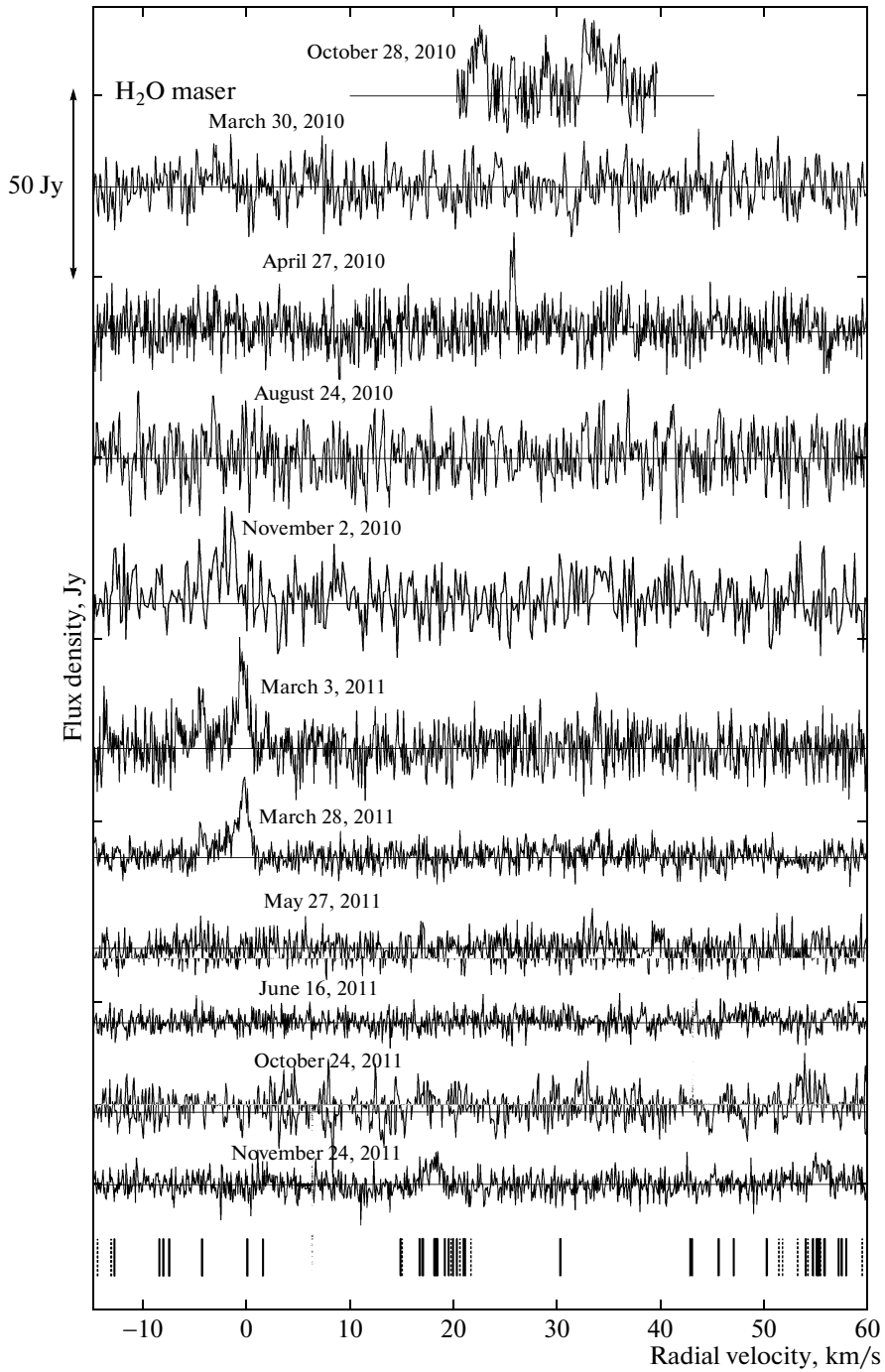


Fig. 1. Spectra of the H_2O maser emission toward W33C. The double arrow shows the scale. The radial velocity is given relative to the LSR. The vertical lines at the bottom mark the velocities at which emission features were observed by us (solid) and other authors (dashed).

2. OBSERVATIONS AND DATA

The observations of the 1.35-cm H_2O maser emission toward W33C ($\alpha_{1950} = 18^{\text{h}}11^{\text{m}}18.3^{\text{s}}$, $\delta_{1950} = -17^{\circ}56'21''$) were carried out on the 22-m Pushchino Radio Astronomy Observatory (PRAO) telescope in November 1981, and then from March

2010 to November 2011. The noise temperature of the system with a cooled front-end FET amplifier was 120–270 K, depending on weather conditions.

The signal analysis was carried out using a 2048-channel autocorrelator with a spectral resolution of 6.1 kHz (0.0822 km/s at 22 GHz). For a point-like

Table 1. Main components of Stokes parameter V in the 1665-MHz line

Date	F_1 , Jy	F_2 , Jy	$ F_1/F_2 $	$\delta V_{2,1}$, km/s	F_3 , Jy	F_4 , Jy	$ F_3/F_4 $	$\delta V_{4,3}$, km/s
December 5, 2008	4.07	-2.07	1.97	1.62	1.4	-1.0	1.4	0.69
April 6, 2010	4.30	-2.2	1.95	1.63	2.3	-0.9	2.56	0.80
July 4, 2010	3.8	-2.2	1.73	1.67	4.3	-1.4	3.07	0.88
January 7, 2011	4.1	-2.3	1.78	1.62	4.3	-2.1	2.05	0.77
May 3, 2011	4.3	-2.2	1.95	1.60	3.0	-0.8	3.75	0.81
July 11, 2011	4.0	-2.2	1.82	1.62	3.1	-0.9	3.44	0.79

source, an antenna temperature of 1 K corresponds to a flux density of 25 Jy [9].

The observations of W33C in the 18-cm hydroxyl lines were conducted on the radio telescope of the Nançay Radio Astronomy Station of the Paris–Meudon Observatory (France) at various epochs. The telescope is a Kraus system two-mirror instrument able to observe radio sources near the meridian. Using a spherical mirror enables tracking of a radio source within $\pm 30^{\text{m}} / \cos \delta$ about the meridian in hour angle, by moving the feed. At declination $\delta = 0^\circ$ the telescope beamwidth at 18 cm is $3.5' \times 19'$ in right ascension and declination, respectively. The telescope sensitivity at $\lambda = 18$ cm and $\delta = 0^\circ$ is 1.4 K/Jy. The noise temperature of the helium-cooled amplifiers is from 35 to 60 K, depending on the observing conditions.

The spectral analysis was conducted using an autocorrelation spectrum analyzer with a frequency resolution of 763 Hz. In the 1665- and 1667-MHz lines, this corresponds to a radial-velocity resolution of 0.137 km/s. In the observations in 2010–2011, the resolution was twice as high, 0.068 km/s. Since 2008, the radio telescope simultaneously receives two perpendicular modes of linear polarization, yielding directly the intensities of the corresponding linear modes ($L 0^\circ$, $L 90^\circ$). Mixing the signals from the perpendicular feeds with a quarter-wavelength phase delay applied to one of the modes produces two orthogonal circular modes (LC, RC). Thus, three Stokes parameters I , V , and Q are observed simultaneously (with an appropriate choice of the coordinate system).

The observations were processed using the GILDAS software package (IRAM, Grenoble, France), available on the Web at <http://www.iram.fr/IRAMFR/GILDAS/> [9].

Figure 1 presents the H₂O spectra for various epochs. The double arrow shows the scale in Jansky. The horizontal axis plots the velocity relative to the Local Standard of Rest (LSR). The vertical bars at

the bottom mark the velocities at which emission features have been observed by either ourselves or other authors [3, 7, 8].

The H₂O maser emission was mostly observed in two spectral intervals: from -7 to +1 km/s and from 32 to 37 km/s (Fig. 2). Single emission features scattered in the spectrum from 9 to 55 km/s were also observed. Thus, the full velocity interval is about 62 km/s.

The results of our observations of the hydroxyl maser emission in the 1665- and 1667-MHz lines at various epochs are shown in Fig. 3. In 1975 and 1978, the observations were carried out with a resolution of 1 km/s, in 2008 with a resolution of 0.137 km/s, and in 2010–2011 with a resolution of 0.068 km/s. The solid and dashed curves show the emission in the left- and right-circular polarizations. The observation technique is described in [10, 11].

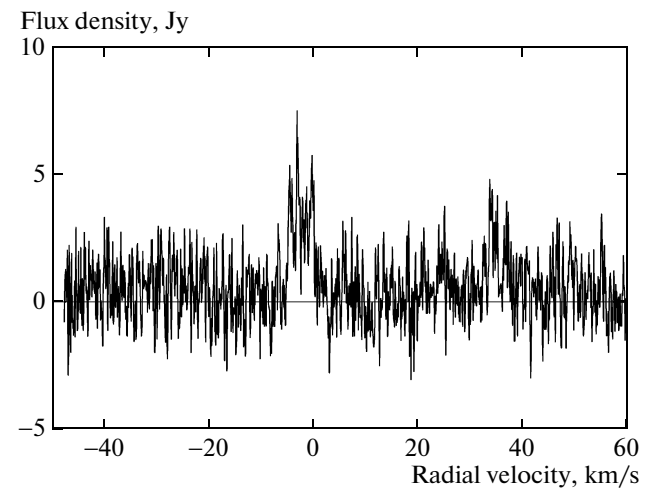


Fig. 2. Averaged spectrum of the W33C H₂O maser emission for 2010–2011.

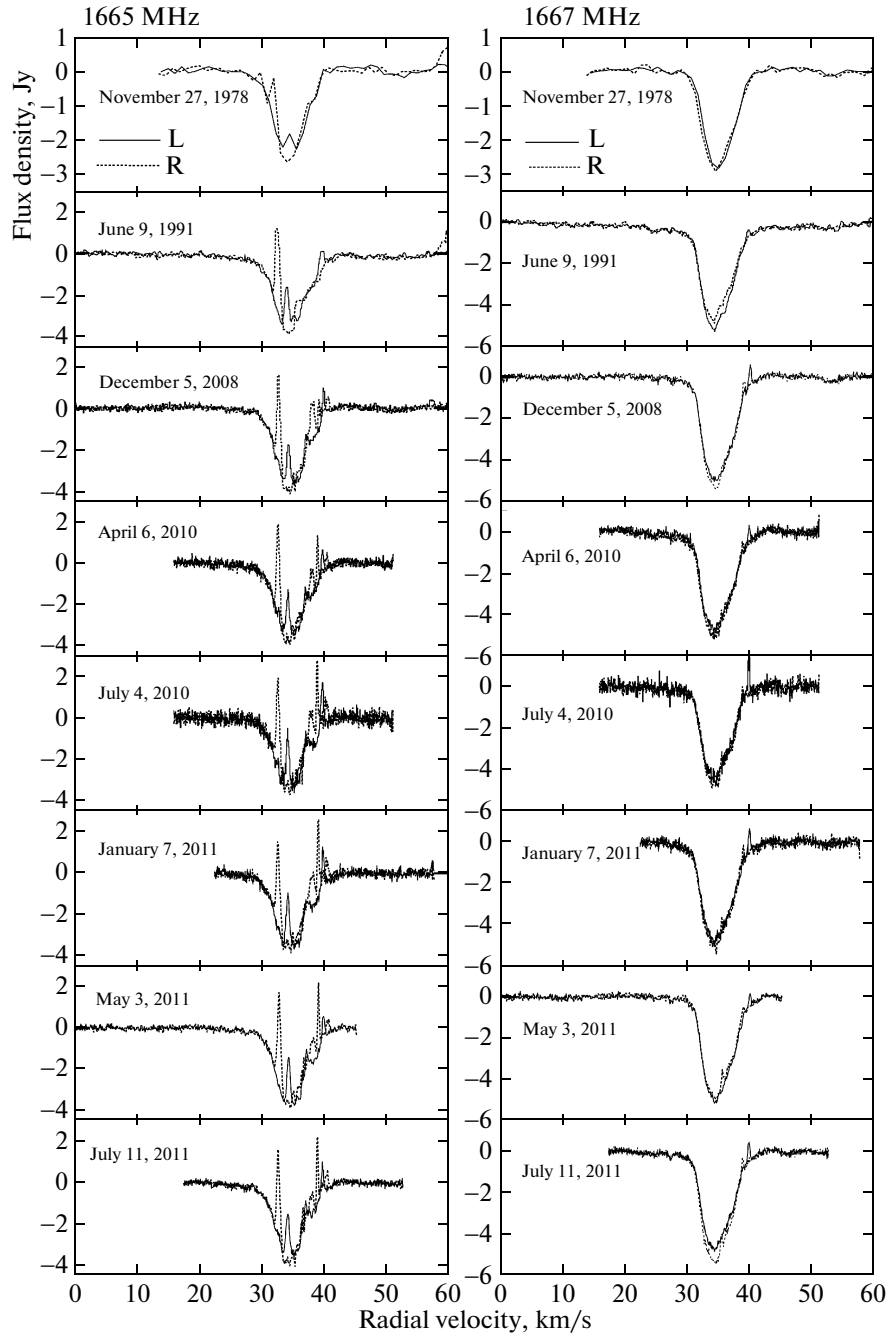


Fig. 3. Spectra of maser emission in the 1665- and 1667-MHz hydroxyl lines for left- (L) and right- (R) circular polarizations at various observing epochs.

The results of the observations in the satellite lines (1612 and 1720 MHz) are shown in Fig. 4.

Figures 5 and 6 show Stokes parameters for the 1665 and 1667 MHz main lines for December 5, 2008, and May 3, 2011. Time variations of Stokes parameter V for the central part of the 1665-MHz spectrum are presented in Fig. 7, and for the 1667-MHz line in Fig. 8. The main components are num-

bered, and their parameters are listed in Tables 1 and 2, where F_1 , F_2 , F_3 , and F_4 are the component flux densities, and $\delta V_{2,1}$ and $\delta V_{4,3}$ are the velocity differences between components 2 and 1 and components 4 and 3.

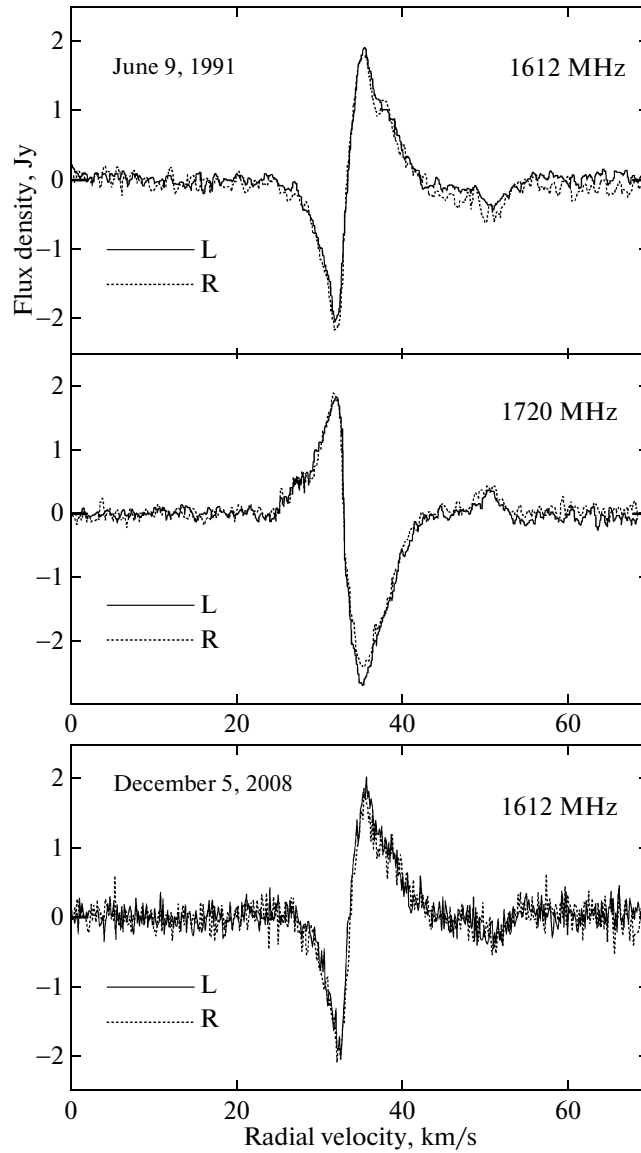


Fig. 4. Same as Fig. 3 for the 1612 and 1720-MHz satellite lines.

3. DISCUSSION OF THE RESULTS

Though the maser source W33C was first discovered long ago, it has been poorly studied in both the water-vapor line and the hydroxyl lines. No high angular resolution observations are available, preventing determination of the spatial locations of the observed emission features. Therefore, our data analysis concentrated on variability of the maser emission.

3.1. H_2O Maser Emission

In spite of the fact that we have conducted regular observations of the H_2O maser emission in G12.8–0.2 only since the beginning of 2010, we

managed to find a number of important peculiarities of this emission. The main ones are listed below.

1. The emission spectrum is fairly broad, from -7 to 55 km/s.
2. Most emission features are short-lived.
3. There are two groups of persistent emission features with a radial-velocity difference of ~ 37 km/s; the mean velocity of the second group (34 km/s) coincides with the central velocity of the OH absorption line and the velocity of the OH maser emission.
4. There is weak emission at 24 km/s, clearly visible after averaging the H_2O spectra (Fig. 2). This suggests this emission is faint but fairly stable.

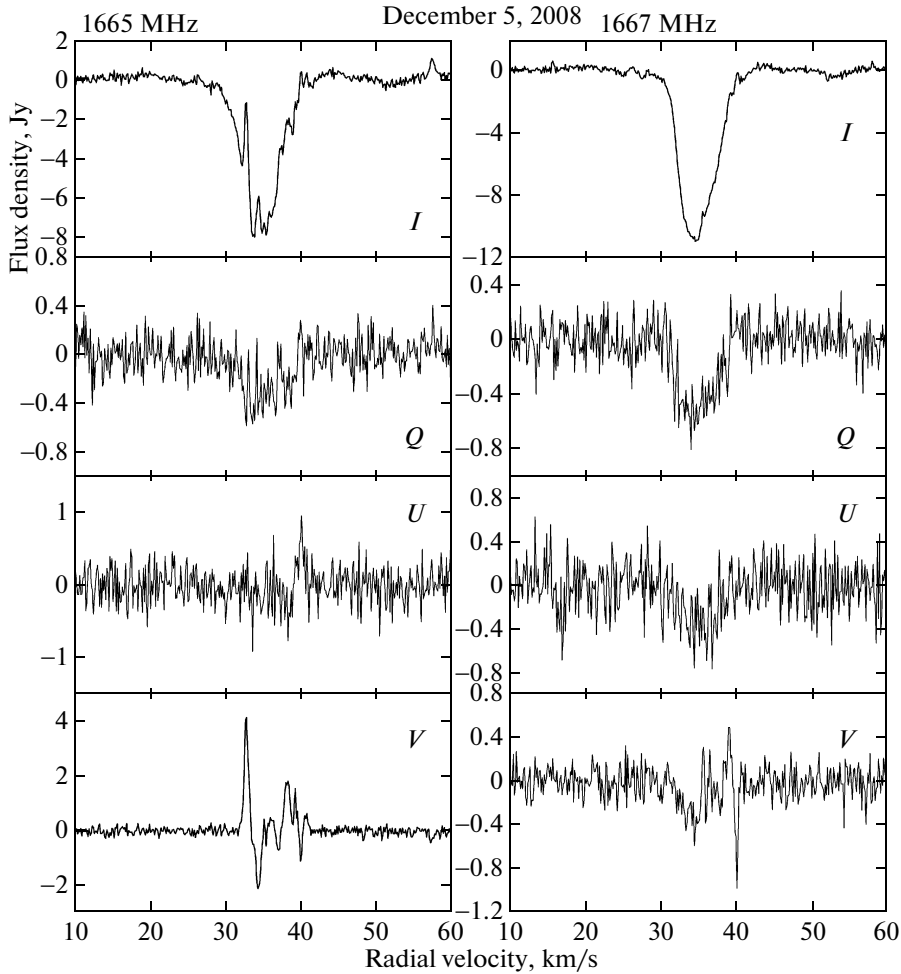


Fig. 5. Stokes parameters for the emission in the 1665- and 1667-MHz hydroxyl lines at epoch December 5, 2008.

In addition to the H₂O spectrum, we have also detected a continuum signal with $T_a \sim 0.5$ K, which corresponds to a flux density of ~ 15 Jy.

3.2. Hydroxyl Emission

We observed strong absorption in all the OH main-line profiles, on which the maser emission was superimposed. The absorption line with a central velocity of 35.8 km/s arises in a compact molecular cloud, which is also a type IIc OH emission source in the 1612- and 1720 MHz lines [2]. The absorption full width at half-maximum is 5.8 km/s.

The variability of the OH maser emission in W33C is most clearly manifested in Stokes parameter V ; therefore, our subsequent analysis is mostly connected with variations of this parameter.

The amplitudes of features 1 and 2 observed only in the 1665-MHz line varied very weakly, whereas features 3 and 4 underwent considerable amplitude

variations in both main lines (Tables 1 and 2). The listed pairs of features arise due to splitting of the emission at 33.4 and 39.4 km/s into two components in a longitudinal magnetic field, which are shifted in velocity up and down and elliptically polarized in opposite directions.

In the 1665-MHz line, the difference in the radial velocities of features 2 and 1 is 1.7 km/s, and between features 4 and 3 it is 0.8 km/s. The splitting of 1.7 km/s in the emission at 33.4 km/s corresponds to a longitudinal magnetic field of 2.9 mG, and a splitting of 0.8 km/s at 39.4 km/s to a field of 1.4 mG.

In the emission detected by us in the 1667 MHz line, the separation between the Zeeman components 4 and 3 is ≈ 1 km/s (Table 2), corresponding to a magnetic field of 2.8 mG. The factor-of-two difference in the magnetic field intensity for the emission at 39.4 km/s found from the splitting in the main OH lines could have various origins. The emission regions could be close but not coincident, or have different

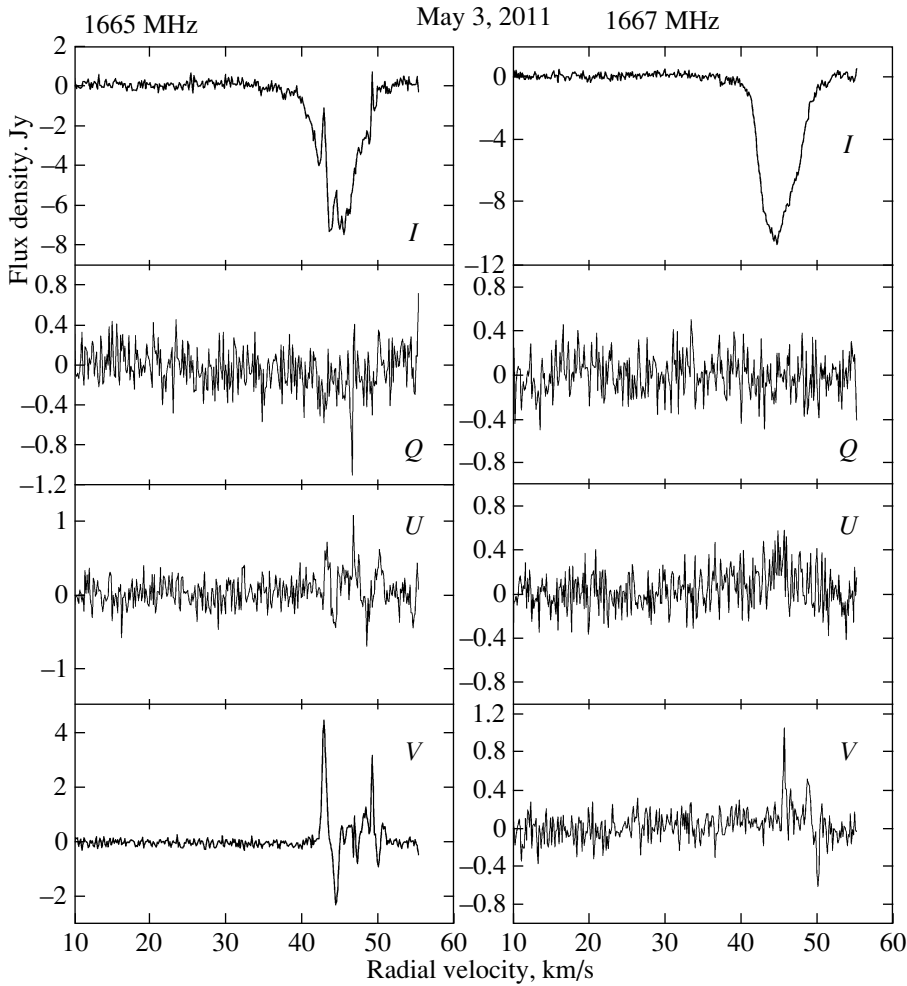


Fig. 6. Same as Fig. 5 for epoch May 3, 2011.

sizes (with the region radiating in the 1667-MHz line being more extended). In both cases, the medium should be inhomogeneous and turbulent.

The profiles of the 1612- and 1720-MHz OH lines (Fig. 4) consist of emission and absorption components and mirror each other. This structure can be explained in the model in which the OH source is associated with a molecular cloud around the maser in the presence of an embedded IR emission source that affects the populations of hyperfine-structure sublevels of the OH molecules [12]. The particulars of the IR pumping in the model [12] are such that the inversion in the 1720-MHz transition is accompanied by an anti-inversion in the 1612-MHz line, and vice versa. Observations of a number of sources in the OH satellite lines [13, 14], indeed, demonstrate mirror line profiles: 1612 MHz in emission, 1720 MHz in absorption, and vice versa. If a magnetic field is present in the cloud, then, according to the model [12], the inversion or anti-inversion of a particular OH

satellite transition is determined by the angle between the direction of propagation of the IR emission and the direction of the local magnetic field. When the source is inside the cloud, inversion in one of the satellite lines and anti-inversion in the other will be observed in some parts of the cloud; in other parts of the cloud, the situation will be reversed. If the cloud is not resolved by the radio telescope beam, the superposition of profiles of satellite lines from different parts of the cloud produces a pattern similar to that in Fig. 4.

3.3. Model of the Maser Source in W33C

Let us summarize the results of our OH and H₂O observations. The hydroxyl emission and the emission of a group of water-vapor features occurs at the same radial velocities (30–40 km/s). Note that the emission in other molecular lines (e.g., CH₃OH [15]) and in radio recombination lines (e.g., H134α [16]) is also observed in this velocity range. All this emission

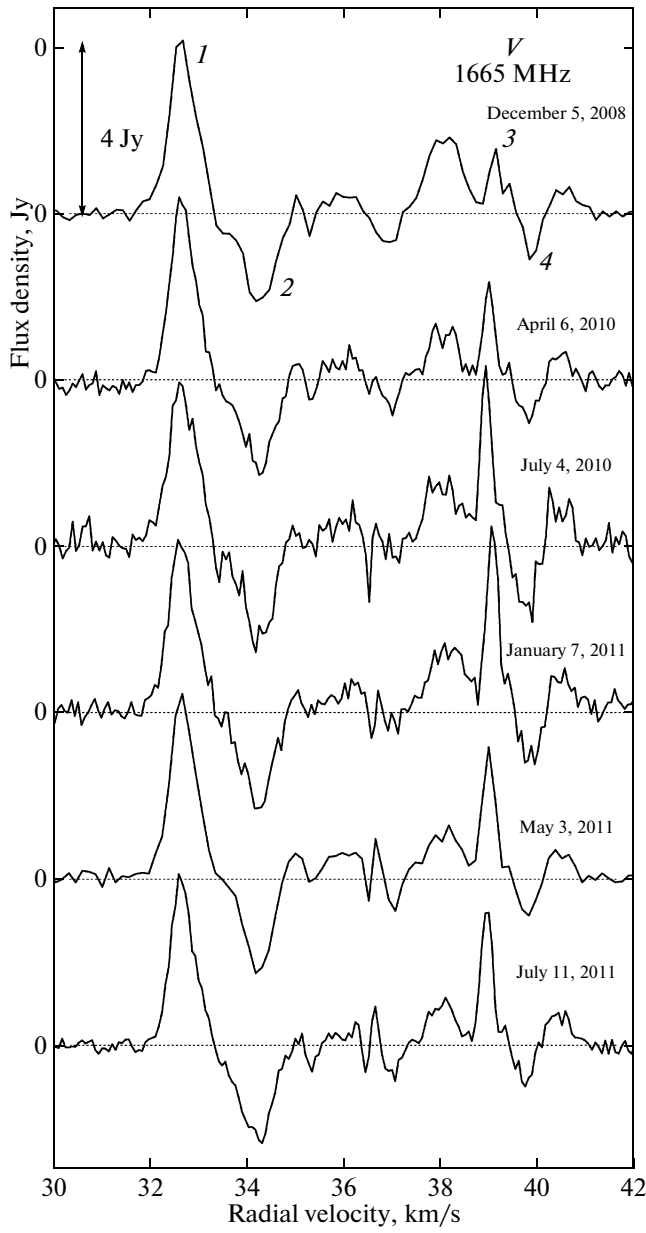


Fig. 7. Time variations of Stokes parameter V for the central part of the 1665-MHz spectrum. The main features are numbered.

is most likely associated with the same molecular cloud at a radial velocity of about 35 km/s.

Note also that the profiles of the hydroxyl and methanol lines have a double-peaked structure, whose components are arranged more or less symmetrically about a velocity of 35 km/s. This structure of the spectra is most easily explained if we are dealing with a rotating molecular cloud. The rotation velocity is low, i.e., the line-of-sight projection of the cloud's rotation velocity is small.

The H_2O line profiles have a different structure (Fig. 1 and 2). The fairly stable emission at velocities

from -7 to 1 km/s and at 24 km/s could be associated with a bipolar outflow.

4. MAIN RESULTS

Let us list the main results of our observations of water-vapor and hydroxyl masers in W33C.

1. We have detected a large number of strongly variable, short-lived H_2O emission features in a broad interval of radial velocities, from -7 to 55 km/s. The velocity of one of the groups with the most stable

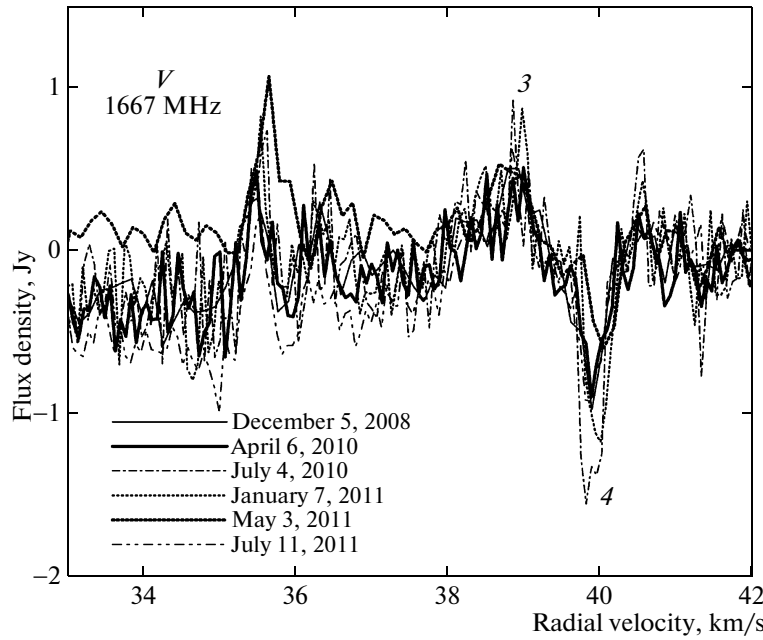


Fig. 8. Same as Fig. 7 for the central part of the 1667-MHz spectrum.

emission (34 km/s) is close to the central velocity of the OH absorption line and OH maser emission.

2. We have detected maser emission of W33C in the 1667-MHz line in both circular polarizations in the velocity interval 35–41 km/s.

3. We have detected Zeeman splitting in the OH 1665-MHz main line for the emission at 33.4 and 39.4 km/s. We have used the amount of splitting to estimate the line-of-sight component of the magnetic field for each of the masing regions at 33.4 and 39.4 km/s (2.8 and 1.4 mG).

4. “Mirror” profiles of the 1612 and 1720 MHz OH satellite lines suggest pumping of the levels of the corresponding transitions by IR emission from a source embedded in a magnetized molecular cloud surrounding the maser.

Table 2. Main components of Stokes parameter V in the 1667-MHz line

Date	F_3 , Jy	F_4 , Jy	$ F_3/F_4 $	$\delta V_{4,3}$, km/s
December 5, 2008	0.50	-0.85	0.59	1.02
April 6, 2010	0.41	-0.76	0.54	0.99
July 4, 2010	0.81	-1.38	0.59	1.02
January 7, 2011	0.79	-1.15	0.69	0.98
May 3, 2011	0.48	-0.57	0.84	1.23
July 11, 2011	0.52	-0.53	0.65	0.96

5. We have observed appreciable variability of the 39.0- and 39.8-km/s Zeeman-splitting components in both main lines; at the same time, the 32.6- and 34.3-km/s components in the 1665 MHz line remained fairly stable, while they were not detected at all in the 1667-MHz line.

6. The extended spectrum and fast variability of the H₂O maser emission, together with the variability of the Zeeman splitting components at 39 km/s in the main OH lines, could be due to composite, clumpy structure of the molecular cloud and the presence of large-scale (rotation, bipolar outflow) and turbulent motions of the material in this cloud.

ACKNOWLEDGMENTS

The RT-22 PRAO radio telescope is supported by the Ministry of Science and Education of the Russian Federation (registration number 01-10). This work was supported by the Russian Foundation for Basic Research (project code 09-02-00963-a). The authors are grateful to the staff of the Pushchino and Nançay radio astronomy observatories for their help with the observations.

REFERENCES

1. M. I. Pashchenko, Astron. Tsirk. No. 886, 1 (1975).
2. M. I. Pashchenko, Sov. Astron. Lett. **6**, 58 (1980).
3. R. Genzel and D. Downes, Astron. Astrophys. Suppl. Ser. **30**, 145 (1977).

4. P. A. Shaver and W. M. Goss, *Austral. J. Phys. Astrophys. Suppl.*, No. 14, 77 (1970).
5. W. M. Goss and P. A. Shaver, *Austral. J. Phys. Astrophys. Suppl.*, No. 14, 1 (1970).
6. V. Radhakrishnan, W. M. Goss, J. D. Murray, and J. W. Brooks, *Astrophys. J. Suppl. Ser.* **24**, 49 (1972).
7. D. T. Jaffe, R. Güsten, and D. Downes, *Astrophys. J.* **250**, 621 (1981).
8. G. Comoretto, F. Palagi, R. Cesaroni, et al., *Astron. Astrophys. Suppl. Ser.* **84**, 179 (1990).
9. M. I. Pashchenko and E. E. Lekht, *Astron. Rep.* **49**, 624 (2005).
10. V. I. Slysh, M. I. Pashchenko, G. M. Rudnitskii, et al., *Astron. Rep.* **54**, 599 (2010).
11. M. I. Pashchenko, G. M. Rudnitskii, and P. Colom, *Astron. Rep.* **53**, 541 (2009).
12. V. V. Burdyuzha and D. A. Varshalovich, *Sov. Astron.* **16**, 597 (1972).
13. M. I. Pashchenko, G. M. Rudnitskii, and O. Franquelin, *Sov. Astron. Lett.* **5**, 276 (1979).
14. R. F. Haynes and J. L. Caswell, *Mon. Not. R. Astron. Soc.* **178**, 219 (1977).
15. A. D. Haschick, K. M. Menten, and W. A. Baan, *Astrophys. J.* **354**, 556 (1990).
16. F. F. Gardner, T. L. Wilson, and P. Thomasson, *Astrophys. Lett.* **16**, 29 (1975).

Translated by G. Rudnitskii